

Second-harmonic generation of a continuous-wave diode-pumped Nd:YAG laser using an externally resonant cavity

W. J. Kozlovsky, C. D. Nabors, and R. L. Byer

Edward L. Ginzton Laboratory, Stanford University, Stanford, California 94305

Received June 19, 1987; accepted September 8, 1987

We report 13% second-harmonic conversion efficiency of a 15-mW, cw, diode-laser-pumped Nd:YAG oscillator. 2 mW of single-axial-mode 532-nm radiation was generated by externally resonant second-harmonic generation in a monolithic MgO:LiNbO₃ nonlinear crystal cavity. The measured finesse of 450 for the monolithic external cavity indicated that absorption and scatter losses in the doubler were less than 0.8%.

The recent development of high-power laser diodes has renewed interest in diode-laser-pumped solid-state lasers. Diode-pumped lasers offer improved reliability, efficiency, and frequency stability¹ compared with lamp-pumped lasers. Second-harmonic generation (SHG) of these infrared laser sources is necessary for many applications. However, the lower power available from diode-pumped lasers makes efficient frequency doubling more challenging than for high-power lamp-pumped lasers.

One demonstrated method for efficient SHG of diode-pumped solid-state lasers is intracavity frequency doubling.² The nonlinear crystal is placed inside the laser resonator to take advantage of the high circulating intensity to produce second-harmonic output efficiently. In these linear laser resonators, however, spatial hole burning usually allows several axial modes to oscillate. Since the losses of these axial modes are coupled through sum-frequency generation in the doubling crystal, the resulting output at the second harmonic is strongly amplitude modulated.³

An alternative approach is resonant external-cavity SHG.⁴ In this method, the nonlinear medium is placed in an external resonator designed to enhance the fundamental field, the second-harmonic field, or both. These resonantly enhanced fields efficiently generate second-harmonic power without the amplitude instabilities seen in intracavity frequency doubling. An additional advantage of external-cavity SHG is that the laser oscillator and the external harmonic resonator can be independently optimized. This is especially important in low-gain or quasi-three-level laser systems.⁵ Independent optimization also permits the design of a single-axial-mode laser source, ensuring that the output of the external doubler is also in a single axial mode.

External-cavity resonant SHG requires the coincidence of the laser and external resonator frequencies. Thus a single-axial-mode, frequency-stable laser oscillator⁶ is important. Diode-pumped, monolithic, nonplanar-ring Nd:YAG lasers^{7,8} are ideal laser sources for external resonant SHG because of their single-mode, frequency-stable output power and their good resistance of feedback.

The nonplanar ring oscillator used for these experiments has been described by Kane *et al.*⁸ It operated TEM₀₀ and in a single axial mode with a linewidth of less than 10 kHz and a drift of less than 1 MHz per minute. It produced 15 mW of cw output power when pumped by a 120-mW diode-laser source.

MgO:LiNbO₃ was chosen for the external doubler because of its low scatter and absorption loss at 1.06 μm (Ref. 9) and its large nonlinear and electro-optic coefficients. Both ends of a 4 mm × 4 mm × 25 mm crystal of MgO:LiNbO₃ were polished with 20-mm radii of curvature and then coated to be 99.7% reflecting at 1.06 μm. This monolithic cavity design provided stability of the resonant frequency and also minimized cavity losses; this is essential for large field enhancements in the external resonator. The cavity geometry with an n_0 of 2.23 yields a cavity beam waist of 38 μm and an axial-mode spacing of 2.7 GHz. The MgO:LiNbO₃ cavity resonant frequency was tuned by applying a voltage across the crystal y axis, using the r_{22} electro-optic coefficient to change n_0 and thereby the optical path length. One free spectral range was scanned with 1040 V.

Figure 1 shows a schematic of the experimental setup. For the doubling experiments, the oven containing the monolithic MgO:LiNbO₃ crystal resonator was heated to the noncritical 90° phase-matching temperature of 107°C. Spatial mode matching into the doubling cavity was accomplished with a 10-cm focal-length lens and proper adjustment to the position and orientation of the harmonic crystal. This was the only mechanical adjustment needed, since the monolithic design ensured alignment of the MgO:LiNbO₃ resonator itself. A Faraday isolator was placed between the laser and the doubler to collect the fundamental radiation backreflected from the doubling crystal, which was a minimum at resonance. On resonance, the high circulating intensity of the fundamental in the doubling crystal efficiently generated the second harmonic. Since the external doubler was a standing-wave resonator, the second harmonic was generated in both directions. The use of two dichroic mirrors allowed both of the harmonic output beams and the transmitted fundamental beam to be measured.

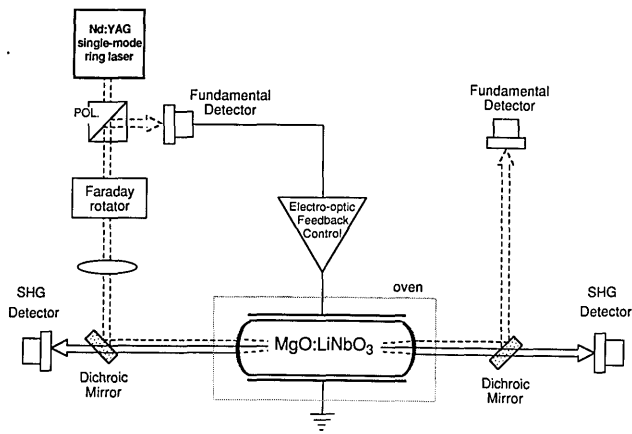


Fig. 1. Experimental setup. The two dichroic mirrors allow the power in both second-harmonic outputs, as well as the transmitted fundamental power, to be measured. The Faraday isolator allows the fundamental power backreflected from the doubling cavity to be detected and therefore to be used for feedback in optimizing resonance. POL, polarizer.

Figure 2 shows the total generated second-harmonic power as a function of incident fundamental power. A commercial scanning confocal interferometer was used to verify that the second-harmonic output was single axial mode. At 15 mW of input power, 2 mW of second-harmonic power was generated, yielding a conversion efficiency of 13%. The bias voltage necessary to maintain resonance drifted slowly, probably as a result of photoconductivity screening the voltage applied across the crystal.¹⁰ Resonance was maintained by a servo loop based on the detection of the reflected fundamental, with a small dither signal applied to the feedback voltage on the doubler. With the cavity locked, the output at the second harmonic had amplitude fluctuations of less than 5%, largely because of technical noise in the servo loop.

With the crystal at room temperature, the harmonic-generation process was not phase matched, so no doubling occurred. The crystal resonator then operated as a high-finesse interferometer. The finesse was measured to be greater than 450, indicating that total losses in the resonator were less than 1.4%. Coating transmittance accounted for 0.6% of this loss, indicating that all other losses were less than 0.8% in a round trip.

The output of the doubler may be calculated by using the external resonator SHG theory of Askin, Boyd, and Dziedzic (ABD).⁴ Because scattering and absorption losses in the crystal are so low, depletion of the resonated fundamental caused by SHG must be considered. This factor is not considered in the theory of ABD but is easily accounted for by an additional loss term that is proportional to the circulating intensity. Let $\eta_{\text{SHG}} = \gamma_{\text{SHG}} P_c$, where η_{SHG} is the conversion efficiency of the resonated fundamental to the second-harmonic power and P_c is the circulating intensity of the fundamental in the doubling cavity. The proportionality factor γ_{SHG} can be derived by using the formalism of Boyd and Kleinman for a focused Gaussian

beam.¹¹ Then $t_{\text{SHG}} = (1 - \gamma_{\text{SHG}} P_c)$ is the fraction of resonated fundamental not converted in a single pass of doubling. Since the second harmonic is generated in both directions, the ABD cavity-reflectance parameter r_m becomes

$$r_m = t^2 t_{\text{SHG}}^2 r_2, \quad (1)$$

where, following ABD conventions, t is the single-pass power transmittance of the crystal, t_1 is the input-mirror power transmittance, and r_2 is the backmirror power reflectance. For a given incident fundamental power P_1 on resonance, then,

$$P_c = \frac{t_1 P_1}{(1 - \sqrt{r_1 r_m})^2}, \quad (2)$$

and the total output at the second harmonic is

$$P_2 = 2\gamma_{\text{SHG}} P_c^2. \quad (3)$$

For our crystal, with $d_{\text{eff}} = 5.95 \times 10^{-12}$ m/V (Ref. 12) and an effective phase-matching length of only 1.3 cm,⁹ $\gamma_{\text{SHG}} = 0.0025/\text{W}$. Figure 2 shows the numerical solution to the above equations plotted as a curve along with the experimental data points. It is interesting to note that the 13% conversion from input fundamental to output second-harmonic power corresponds to an internal conversion efficiency (or effective loss to the circulating intensity) of only 0.3% and a circulating intensity of 620 mW.

The circulating intensity can also be determined by measuring the fundamental power transmitted through mirror r_2 . Figure 3 shows the transmitted fundamental power versus incident power with and without doubling. The line is the theory, and the squares are the data. The excellent agreement between theory and data indicates that all losses of the resonator, including doubling, are properly determined. The lower circulating intensity while the crystal is phase matched corresponds to a reduction in the Q of the cavity due to doubling and also to the decrease of fundamental power coupled into the resonator because of the changing reflectance parameter. During SHG, the measured fundamental power throughput

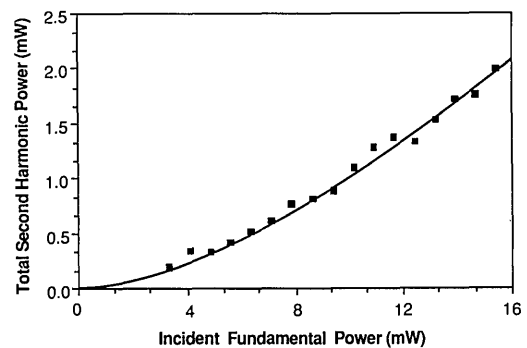


Fig. 2. Total second-harmonic power versus incident power at the fundamental. The squares are experimental data, and the line is theory. The nonparabolic output is expected theoretically, since the coupling efficiency into the resonator changes with increasing second-harmonic conversion.

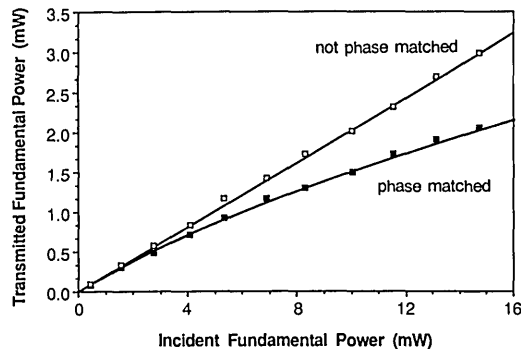


Fig. 3. Transmitted fundamental power as a function of incident power at the fundamental. The transmitted fundamental is directly proportional to the circulating power in the resonant doubler and can be used for comparison with theory.

and the fundamental power reflected from the resonator totaled 8 mW of the 15-mW incident power.

As stated in ABD, it is possible to couple into the external resonator perfectly and not to reflect any of the incident fundamental power (i.e., to impedance match) by choosing the input mirror reflectance r_1 to equal the reflectances parameter r_m . Therefore a simple change of mirror reflectances could resonate all the incident fundamental power, so the conversion efficiency would approach 40% at 15 mW of input power. The performance could also be improved by replacing the standing-wave resonator with a monolithic ring resonator. Such a device would provide single-direction second-harmonic output power and would not retroreflect the input beam into the laser resonator, thus eliminating the need for an isolator.

One possible use for the single-frequency second-harmonic power generated by the external resonant doubler would be to frequency stabilize the diode-pumped solid-state laser by locking to a sub-Doppler absorption feature of $^{127}\text{I}_2$.¹³ By adjusting the laser temperature, we were able to tune the doubler output across a Doppler-broadened line in an I_2 cell and observe bright fluorescence, indicating the possibility for a saturation spectroscopy stabilization experiment.

In conclusion, we have demonstrated 13% total second-harmonic conversion efficiency from a cw input of 15 mW at 1.064 μm . The measured finesse of the monolithic $\text{MgO}:\text{LiNbO}_3$ doubling cavity was greater than 450, indicating total resonator losses of less than 1.4%. The doubling-cavity resonance was electro-optically locked to the laser frequency by maintaining a minimum in the reflected fundamental power. The observed high conversion efficiency from a low-power cw input and the single-axial-mode, frequency-stable output demonstrated the advantages of externally resonant harmonic generation.

This research was supported by the U.S. Army Research Office and NASA. W. J. Kozlovsky and C. D. Nabors gratefully acknowledge support of the Fannie and John Hertz Foundation. We thank Crystal Technology for providing the $\text{MgO}:\text{LiNbO}_3$.

References

1. B. Zhou, T. J. Kane, G. J. Dixon, and R. L. Byer, *Opt. Lett.* **10**, 62 (1985).
2. T. Y. Fan, G. J. Dixon, and R. L. Byer, *Opt. Lett.* **11**, 204 (1986).
3. T. Baer, *J. Opt. Soc. Am. B* **3**, 1175 (1986).
4. A. Askin, G. D. Boyd, and J. M. Dziedzic, *IEEE J. Quantum Electron.* **QE-2**, 109 (1966).
5. T. Y. Fan and R. L. Byer, *IEEE J. Quantum Electron.* **QE-23**, 605 (1987).
6. T. J. Kane and R. L. Byer, *Opt. Lett.* **10**, 65 (1985).
7. W. R. Trutna, Jr., D. K. Donald, and M. Nazarathy, *Opt. Lett.* **12**, 248 (1987).
8. T. J. Kane, A. C. Nilsson, and R. L. Byer, *Opt. Lett.* **12**, 175 (1987).
9. J. L. Nightingale, W. J. Silva, G. E. Reade, A. Rybicki, W. J. Kozlovsky, and R. L. Byer, *Proc. Soc. Photo-Opt. Instrum. Eng.* **681**, 20 (1987).
10. A. Cordova-Plaza, M. J. F. Dignonnet, and H. J. Shaw, *IEEE J. Quantum Electron.* **QE-23**, 262 (1987).
11. G. D. Boyd and D. A. Klienman, *J. Appl. Phys.* **39**, 3597 (1968).
12. S. K. Kurtz, J. Jerphagnon, and M. M. Choy, in *Landolt-Börnstein Numerical Data and Functional Relationships in Science and Technology* (Springer-Verlag, Berlin, 1979), p. 673.
13. P. Esherick and A. Owyong, *J. Opt. Soc. Am. B* **4**, 41 (1987).